Springer

Journal of
Mechanical
Science and
Technology

Journal of Mechanical Science and Technology 23 (2009) 124~135

www.springerlink.com/content/1738-494x
DOI 10.1007/s12206-008-1003-7

Diagnosis of mechanical pumping system using neural networks and system parameters analysis †

Tai-Ming Tsai* and Wei-Hui Wang

Department of Systems Engineering and Naval Architecture, National Taiwan Ocean University, 2 Pei-Ning Road, Keelung 20224, Taiwan

(Manuscript Received July 3, 2007; Revised August 18, 2008; Accepted October 14, 2008)

Abstract

Normally, a mechanical pumping system is equipped to monitor some of the important input and output signals which are set to the prescribed values. This paper addressed dealing with these signals to establish the database of input-output relation by using a number of neural network models through learning algorithms. These signals encompass normal and abnormal running conditions. The abnormal running conditions were artificially generated. Meanwhile, for the purpose of setting up an on-line diagnosis network, the learning speed and accuracy of three kinds of networks, *viz.*, the backpropagation (BPN), radial basis function (RBF) and adaptive linear (ADALINE) neural networks have been compared and assessed. The assessment criteria of the networks are compared with the correlation result matrix in terms of the neuron vectors. Both BPN and RBF are judged by the maximum vector based on the post-regression analysis, and the ADALINE is judged by the minimum vector based on the least mean square error analysis. By ignoring the neural network training time, it has been shown that if the mechanical diagnosis system is tackled off-line, the RBF method is suggested. However, for on-line diagnosis, the BPN method is recommended.

Keywords: Neural network; System diagnosis; Correlation analysis; Sensitivity analysis; Radial basis function method; Backpropagation method; Adaptive linear method

1. Introduction

Mechanical system fault detection and diagnosis can be performed by using artificial neural network (ANN) based on the measurements of system parameters. There are two commonly used ANN methods: model-based and pattern recognition. The model-based fault diagnosis (MBFD) technique has been applied to resolve the computational complexity problem in the neural network methodology (Parten et al., 1991) [1]. Recently, the back-propagation neural network (BPNN) was used as the backbone to determine if any abnormality existed in the etching process of the semiconductor manufacturing process by Chen et al., 2006 [2]. A new identification technique for monitoring the dynamic behavior of a structural system subjected to earthquakes by combining a neural network and genetic algorithm has been considered by Chang, 2003 [3]. In the aspect of vibration signals or spectra by way of ANN, utilizing the abnormal vibration spectra of rotating machine test bench to diagnose the system performance in BPNN by Nam and Lee was done in 1992 [4]. The vibration signature recognition of rotating machine fault identification by using BPNN was addressed by Chow et al., 1993 [5]. Fault diagnosis in rotating machinery was performed by Priddy et al., 1993, who were also applying the MBFD technique by using the vibration mode measurement data [6]. Medical imaging using ANN has been shown by Pattichis et al., 2001 to be promising [7]. The pattern recognition of the adaptive linear neural network (ADALINE) method has been ad-

† This paper was recommended for publication in revised form by Associate Editor Seong-Wook Hong

* Corresponding author. Tel.: +886 2 2462 2192 ext. 7113, Fax.: +886 2 2463 3765
E-mail address: mettsai@mail.ntou.edu.tw

dressed and used to identify the alphabetical characters by Tzeng and Juang, 2002. [8] A similar ANN technique for person identification was presented by Zhang et al., 2004 [9]. The application of the ANN technique for image detection has also been addressed by Young et al., 2004, where they considered the target detection problem by mapping these image gradient vectors using linear transformations [10]. Therefore, it is worth exploring the ANN technique to check the parameter clustering image of pump systems for the purpose of diagnosis. Recently, the radial basis function (RBF) neural network has been extensively applied in the areas of the output response analyses and fault diagnosis of analog systems (Cheng et al., 2004) [11]. The effectiveness of the RBF method has been compared with the other techniques by Liang et al., 2001 and the RBF technique showed excellent performance. Singla et al., 2007 have considered a new algorithm for RBF networks in which the concepts of direction-dependent scaling, shaping, and rotation of Gaussian basis functions have been introduced for maximal trend sensing with minimal parameter representations for input output approximation [12-13]. Hsu, 2005 applied both the neural network method and statistical regression method to identify the stock index appropriately [14]. Owing to these proper diagnosis results, one may be inspired to apply the algorithm combining ANN and regression for system diagnostics.

ANN has been proven to be a viable technique applicable in classification problems such as speech recognition, medical diagnosis, handwriting recognition, image processing, and fault diagnosis. Nevertheless, to raise the operation efficiency and availability, it is important to develop a simple and acceptable conventional method to monitor and diagnose the operation performance of a mechanical pumping system in a marine power plant. The easiest way is via examining the input and output model parameters of a mechanical system by using the integrated neural network pattern recognition technique. In this article, we have proposed a new diagnosis methodology for a mechanical system where minimal significant parameters were considered. For the diagnosis of the mechanical pumping systems onboard a modern merchant ship using ANN, three feed-forward neural networks algorithms together with parameter identification were proposed in this study. A motor-driven circulating pumping system has been selected as an example of the onboard marine engine system to monitor and diagnose its operation behaviors. Comparisons of the training time and the diagnosis results of the three ANN algorithms, namely, BPNN, RBF, and ADALINE that applied to the on-line and off-line diagnosis, are discussed. Also, sensitivity analysis is used to quantify and ascertain the most sensitive observable parameter by analyzing their signal-noise end with period.

2. Diagnosis theory

2.1 Correlation analysis for parameter identification

The purpose of correlation analyses to all system parameters is to identify the relative significant and influential parameters for a normal or abnormal system behavior. This can be accomplished by the identification of correlation coefficients. The correlation coefficient is a measure of the relation between two variables. Normally, the correlation coefficients are normalized and range from -1.00 to +1.00. The value -1.00 represents a perfect negative correlation, while a value +1.00 represents a perfect positive correlation. A value 0.00 represents a non-correlation between the two variables. The most widely used form of the correlation coefficient is Pearson's coefficient r, which gives the magnitude and direction of the two associated variables in an interval with ratio scale. Pearson's coefficient r is also referred to as the linear or product-moment correlation and is defined by:

$$r=\frac{N\sum xy-(\sum x)(\sum y)}{\sqrt{[N\sum x^2-(\sum x)^2][N\sum y^2-(\sum y)^2]}} \tag{1}$$

where N is the number of measurement pairs $\boldsymbol{x}$ and $\boldsymbol{y}$.

In addition to the correlation analyses of parameters, the fuzzy logic clustering reasoning and statistical box-plot of measurements for all prescribed running conditions of a mechanical system are conducted simultaneously to ascertain the effective and significant parameters for the proposed exploration conditions. The box-plot is a graphical method based on robust statistics to show the categorization of measurement data population. Besides, data clustering can be used to classify the measurement data into different groups by means of fuzzy c-means (FCM).

The reason to adopt a box-plot is its ability to resist the presence of outliers of measurement data better than the classical statistics based on the normal distri-

bution. The content in the box-plot consists simultaneously of the minimum and maximum of the measurement data, the median values of the first 25%, 50% and 75% measured time-series data. In addition, the outliers encompass either the measurement data larger than the median value of the 75% measured time-series data and the data less than the median value of the first 25% measured time-series data.

FCM allows the measured data to be categorized into clusters by the clustering center-means vectors. This clustering method has been used frequently for pattern recognition. FCM is based on an iterative minimization procedure of the following dissimilarity (or distance) function (J_m) for a collection of N vectors into C groups (or clusters):

$$\boldsymbol{J_m} = \sum_{i=1}^{N}\sum_{j=1}^{C} \boldsymbol{u_{ij}^m}\left\|\boldsymbol{x_i} - \boldsymbol{c_j}\right\|, \quad 1 \le m < \infty \tag{2}$$

where J_m is the distance function of m^{th} iteration, m is any integer number greater than 1, u_{ij} is the value of the membership function of x_i in the j^{th} cluster, x_i is the i^{th} measured data, c_j is the center of the j^{th} cluster, and $\left\|\boldsymbol{x_i} - \boldsymbol{c_j}\right\|$ is the norm of $\left(\boldsymbol{x_i} - \boldsymbol{c_j}\right)$. The fuzzy clustering is carried out through an iterative optimization of the objective function given by Eq. (2) with the update membership function u_{ij} and the cluster centers c_j defined as:

$$u_{ij}^m = \frac{1}{\sum_{k=1}^{C}\left(\frac{\left\|x_i - c_j\right\|}{\left\|x_i - c_k\right\|}\right)^{\frac{2}{m-1}}}, \quad c_j = \frac{\sum_{i=1}^{N} u_{ij}^m \cdot x_i}{\sum_{i=1}^{N} u_{ij}^m} \tag{3}$$

This iteration will stop when $\max\left\{\left|u_{ij}^{(k+1)} - u_{ij}^{k}\right|\right\} < \varepsilon$, where ε is a termination criterion whose value ranges between 0 and 1, whereas k is the index of iteration step. Normally, this procedure converges to a local minimum or a saddle point of $\boldsymbol{J_m}$.

As a summary, the FCM algorithm is composed of the following steps:

Step 1. Initialize $\boldsymbol{U^{(k)}} = [\boldsymbol{u_{ij}}]$ matrix, $\boldsymbol{U^{(0)}}$

Step 2. At the k^{th}-step: calculate the center vectors $\boldsymbol{C^{(k)}} = [\boldsymbol{c_j}]$ with $\boldsymbol{U^{(k)}}$, in which $\boldsymbol{c_j} = \dfrac{\sum_{i=1}^{N} \boldsymbol{u_{ij}^m} \cdot \boldsymbol{x_i}}{\sum_{i=1}^{N} \boldsymbol{u_{ij}^m}}$

Step 3. Update $\boldsymbol{U^{(k)}}$ and $\boldsymbol{U^{(k+1)}}$, in which

$$\boldsymbol{u_{ij}} = \frac{1}{\sum_{k=1}^{C}\left(\frac{\left\|\boldsymbol{x_i} - \boldsymbol{c_j}\right\|}{\left\|\boldsymbol{x_i} - \boldsymbol{c_k}\right\|}\right)^{\frac{2}{m-1}}}$$

If $\left\{\left|\boldsymbol{U^{(k+1)}} - \boldsymbol{U^{(k)}}\right|\right\} < \varepsilon$ then STOP; otherwise return to step 2.

2.2 Neural network models and learning algorithm

An ANN is a set of interconnected groups of artificial neurons that are linked by a mathematical model for information processing. In most cases, ANN is an adaptive system that can change the system's structure based on the external or internal information flowing through the network. In more practical terms, neural networks are non-linear statistical data modeling tools that can be used to establish complex relationships between inputs and outputs and find the patterns amongst data. There are numerous algorithms available for training neural network models. Most algorithms used for training ANN employ the gradient descent method. There are three major learning networks: supervised learning, unsupervised learning and reinforcement learning. Usually, any special type of neural network is accompanied by a special learning method. In this paper, two kinds of supervised learning neural networks, BPN and RBF, and one unsupervised learning neural network, ADALINE, are adopted to create the database of the normal and abnormal prescribed conditions of a mechanical system based on measurements.

Furthermore, there are two kinds of BPN, the feed-forward backpropagation neural networks (FBPN), and the cascade feed-forward backpropagation neural networks (CFBPN). Both FBPN and CFBPN are trained by backpropagation learning method. Normally, the backpropagation learning method is most useful for feed-forward networks. Both of them have multi-layer networks with a number of R inputs and T outputs. But the number of neurons in the hidden layer for FBPN and CFBPN is different.

The two kinds of the BPNs are trained by the number of epochs to generate an individual neural network. The Widrow-Hoff (or least mean square (LMS)) learning algorithm has been used for the training process and generation of the BPN models. With these models, the simulation results can be used to compare with the corresponding measurements to validate and select the most suitable model for describing the running behavior. Fig. 1 shows the detailed architecture of FBPN, in which the sum of the weighted inputs and the input bias form the input in

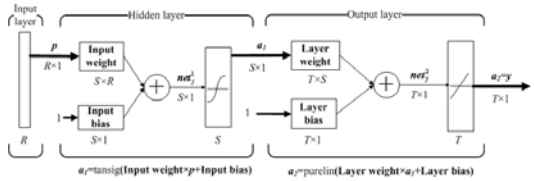

Fig. 1. Network architecture of FBPN.

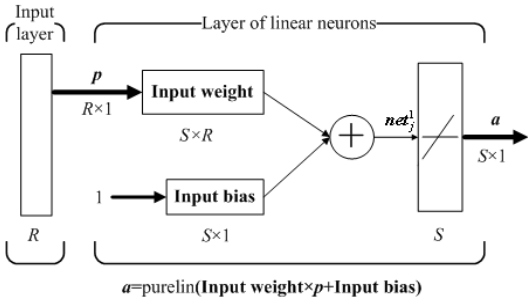

Fig. 2. Network architecture of ADALINE.

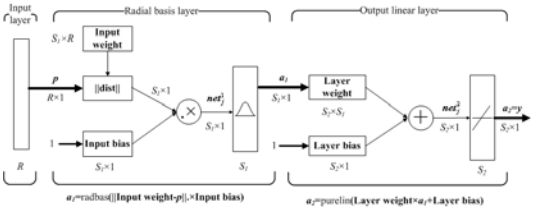

Fig. 3. Network architecture of RBF.

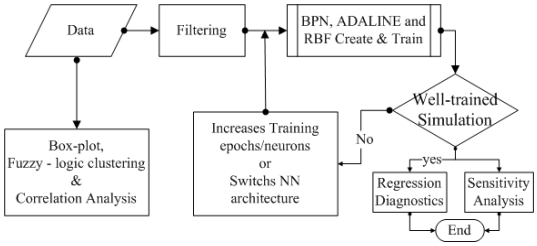

Fig. 4. Diagnostic flow chart for mechanical system.

the tan-sigmoid transfer function f_1 in the hidden layer. The range of the outputs of f_1 is from -1 to +1. The output value becomes the input of the linear transfer function (purelin) f_2, in the output layer. The output of f_2 can be any real number between $-\infty$ and $+\infty$.

Thus, summarizing the above-mentioned description, the mathematical form of the BPN learning algorithm can be derived as follows: Denote $\boldsymbol{p}$ to be an initial input measurement vector of the significant system parameters, a_j^{n-1} to be the output of the j^{th} neuron in the $(n-1)^{th}$ hidden layer and a_j^n to be the output of j^{th} neuron in the n^{th} layer (or the output layer). The relations for $\boldsymbol{p}$, a_j^{n-1} and a_j^n can be expressed as:

$$\boldsymbol{p} = a_j^0 \tag{4}$$

$$a_j^n = \mathrm{f}(net_j^n) \tag{5}$$

And

$$net_j^n = \sum_i w_{ij} a_j^{n-1} - \theta_j \tag{6}$$

where w_{ij} and θ_j are the layer weight and the layer bias of j^{th} neuron in the i^{th} layer respectively. The tan-sigmoid function in the hidden layer is defined by

$$\mathrm{f}_1(net_j^1) = \frac{1}{1+e^{-(net_j^1)}}, j=1,\cdots,S \tag{7}$$

whereas the linear function in the output layer has to attain the output value and is defined by

$$\mathrm{f}_2(net_j^2) = net_j^2, j=1,\cdots,T \tag{8}$$

The ADALINE neural network possesses only the input and linear neuron layers in the architecture as shown in Fig. 2. The input of ADALINE comes from the clustering image of the measured data vectors in the state space of a system. ADALINE is trained adaptively by a number of epochs with the use of LMS to acquire the neurons with least mean square error and to generate the most suitable neural network model for representing the system behavior. Basically, the learning algorithm of ADALINE network can be expressed as:

$$\begin{aligned} w(\mathrm{k}+1) &= w(\mathrm{k}) + 2\alpha e(\mathrm{k}) p^T(\mathrm{k}) \\ b(\mathrm{k}+1) &= b(\mathrm{k}) + 2\alpha e(\mathrm{k}) \end{aligned} \tag{9}$$

where e and b represent the error vector and bias vector, respectively, and w is the weight, p is the

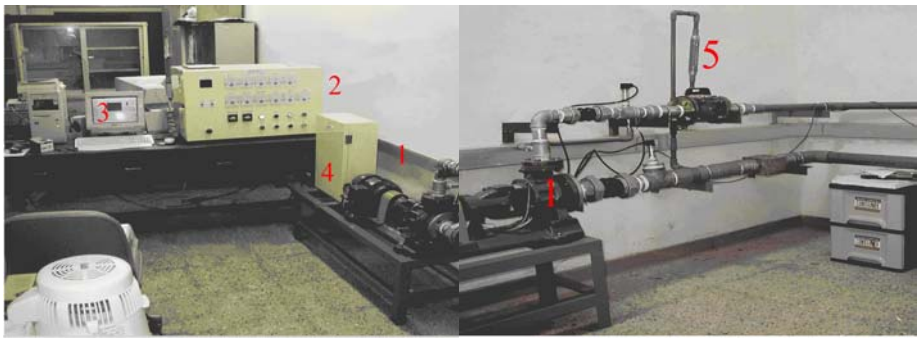

Fig. 5. Layout of experimental set up, 1: Pump Set, 2: Control Panel, 3: Labview Program, 4: Transducer unit, and 5: Air-in Control Valve.

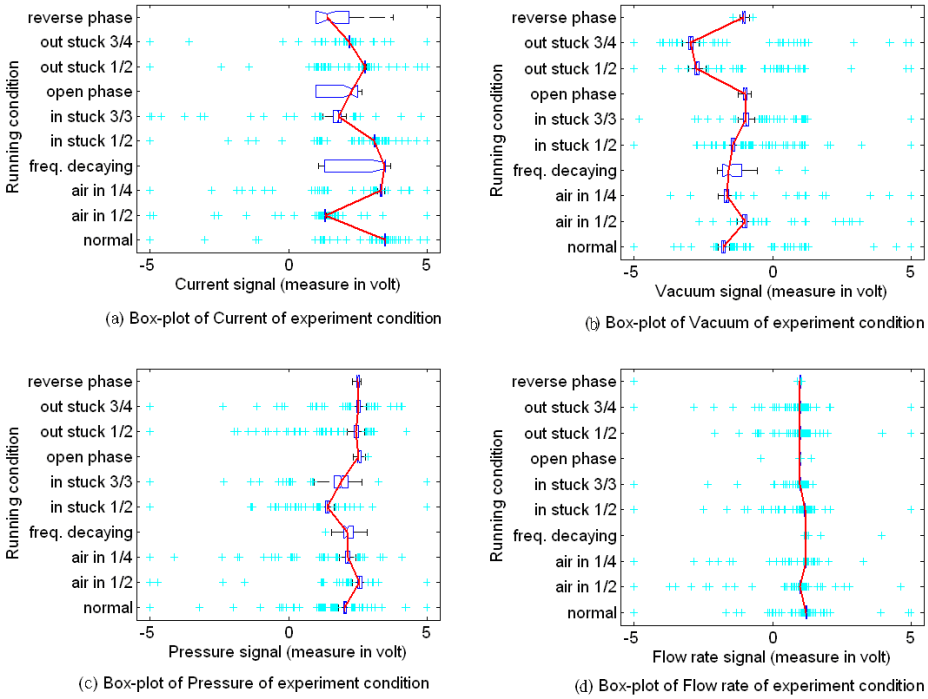

(a) Box-plot of Current of experiment condition

(b) Box-plot of Vacuum of experiment condition

(c) Box-plot of Pressure of experiment condition

(d) Box-plot of Flow rate of experiment condition

Fig. 6.Box-plots of system parameters for each system sampling condition.

input vector, and α is the learning rate.

The RBF neural network also has multi-layers in its architecture, as shown in Fig. 3. The input layer and output linear layer have the same number of neurons as that of BPN. However, the transfer function used in the hidden layer is that of a Gaussian function. Owing to the usage of the Gaussian function, one can produce a significant nonzero response even when the input value is very small. Therefore, the RBF network is sometimes referred to as the localized field receptive network (Hush, 1993) [15]. The number of S_1 neurons in the hidden layer increases as the input data increases progressively. In the radial basis layer of Fig.3, the input vector $\boldsymbol{p}$ of dimension $R\times 1$ and the input weighting matrix ($S_1\times R$) are combined to form the Euclidean distance $\|\boldsymbol{dist}\|$, where dist is the Euclidean distance vector. The Euclidean distance between two points $\boldsymbol{x}_i$ and $\boldsymbol{y}_i$, where i=1,⋯, n in an n-dimensional space is defined by:

$$\|\boldsymbol{dist}\| = \sqrt{(x_1-y_1)^2+(x_2-y_2)^2+\cdots+(x_n-y_n)^2} = \sqrt{\sum_{i=1}^{n}(x_i-y_i)^2} \tag{10}$$

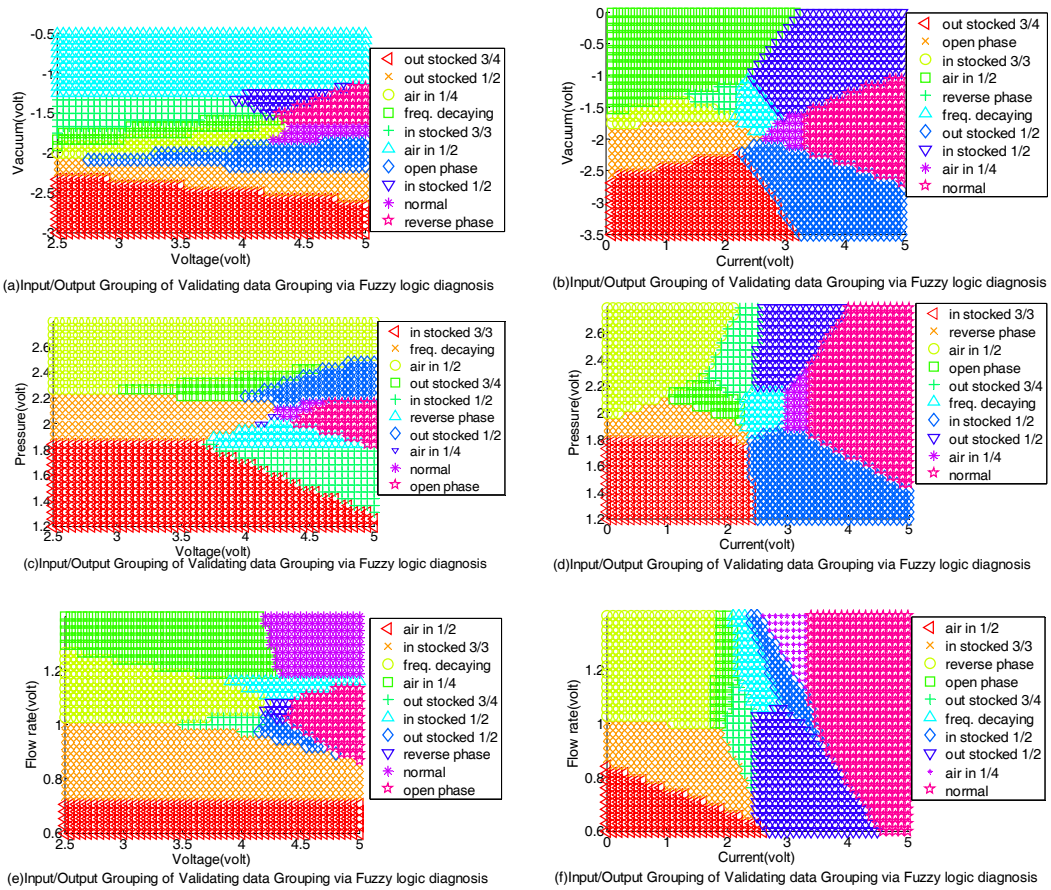

Fig. 7. Fuzzy-logic clustering of parameters by FCM for each system sampling condition.

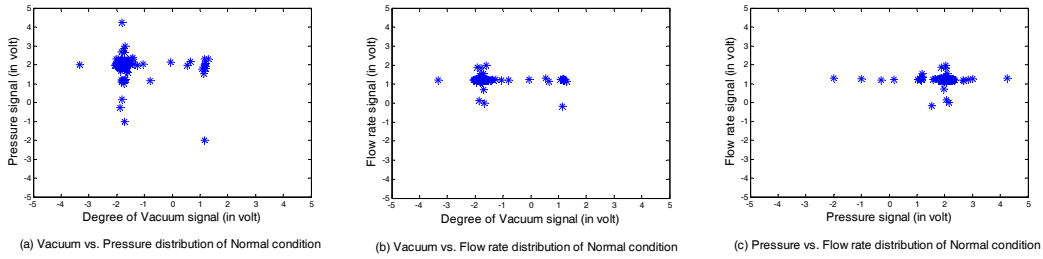

Fig. 8. Clustering image of measured data pair in state space on normal condition of mechanical system.

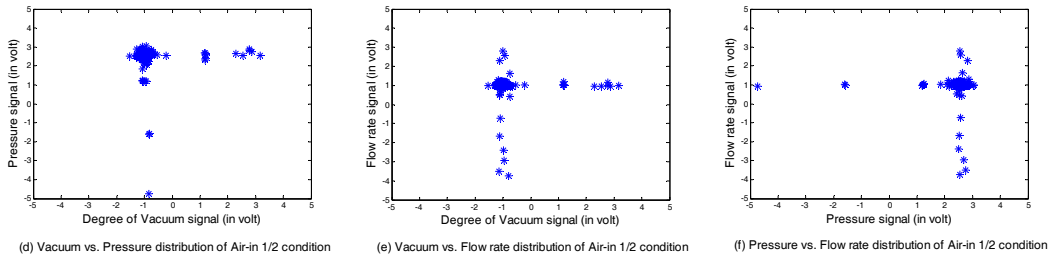

Fig. 9. Clustering image of measured data pair in state space on Air-in 1/2 condition of mechanical system.

ing matrix and the bias vector by using the gradient descent optimization technique, the RBF learning algorithm can attain a well-trained neural network model. The function of the output linear layer in Fig. 3 is to generate the value of output to be any value between $-\infty$ and $+\infty$ through the linear purelin function.

2.3 Regression diagnostics

By the ANN learning algorithm, well-trained simulation results of the normal condition and a number of prescribed abnormal system conditions can be attained. The process of regression diagnostics is to compare a set of measured system signals with the simulation results database for various prescribed running conditions to ascertain the measured signals pertaining to or close to which condition of the system. The judgment criterion is based on the magnitude of the correlation coefficient or network mean square error. When the correlation coefficient resulting from the post linear regression analysis for BPN or RBF is at maximum, then the neural network corresponding to the running condition of this maximum correlation coefficient can be identified for diagnosis purposes. However, when the mean square error for the network ADALINE is at minimum, then the neural network corresponding to the running condition of this minimum mean square error can likewise be identified for diagnosis.

To integrate all the analyses and training processes of the neural network the diagnosis flow chart for mechanical systems in this study is planned as shown in Fig. 4.

2.4 Sensitivity analysis for diagnosis

To identify the most sensitive output parameter of a mechanical system in the fault diagnostic process, sensitivity analysis can be carried out by means of SNR (Piche, 1995) of the system response signal, y and given as: [16]

$$SNR = \frac{\sigma_y^2}{\sigma_{\Delta y}^2} \tag{11}$$

where $\sigma_y^2, \sigma_{\Delta y}^2$ are the variances of $\boldsymbol{y}$ and $\Delta \boldsymbol{y}$ respectively, and $\Delta \boldsymbol{y}$ represents the variation of signal $\boldsymbol{y}$.

3. Diagnosis experiments and discussion

3.1 Experimental set-up of pumping system

The experimental set-up of a motor-driven circulating pumping system is arranged as shown in Fig. 5. Such an arrangement encompasses a 3-phase 220 volt AC induction motor which drives a centrifugal pump and a set of water circulation piping system. The input/output pipe diameter is 2.5/1.5 inches. Twelve sensors and seven fault signal generators were adopted to constitute this mechanical system. The sensors are "power factor" (PF), "voltage", "current", "watt", "rpm" for motor site, "vacuum", "pressure", "flow rate" for pump site, and "temperature" in pump site and working fluid site and "vibration" measured in the shaft and foundation. Ten sampling conditions, one normal and nine fault conditions, with eight sampling channels were considered in this study, which are described as follows and summarized in Table 1.

Normal Condition:

Condition 1: Pumping system was operating in normal condition.

Mechanical fault Conditions: Pumping system was operating abnormally with the following prescribed mechanical fault conditions.

Condition 2: Air leakage valve was opened 1/2 manually.

Condition 3: Air leakage valve was opened 1/4 manually.

Condition 5: Inlet valve was shut 1/2 manually.

Condition 6: Inlet valve was shut off manually.

Condition 8: Outlet valve was shut 1/2 manually.

Condition 9: Outlet valve was shut 3/4 manually.

Electrical fault Conditions: Motor-driven pump had the following electrical faults at the power source.

Condition 4: Frequency of power source decayed rapidly.

Condition 7: One of the three phases of AC power was broken.

Condition 10: Phase sequence of AC power reversed manually.

In the diagnosis experiment of the set up pumping system, all the signals were measured by NI 6024E DAQ card with Labview code and the measurement data were analyzed with Matlab software.

3.2 Box-plot, fuzzy-logic clustering and correlation analysis

The eight parameters for the diagnosis of the

pumping system are power factor, voltage, current, power, RPM of motor, degree of vacuum, pressure at the pump outlet and flow rate. The relation between power factor (P_f), voltage and current is defined by the inverse cosine function:

$$P_f = \cos^{-1}\left(\frac{Power}{Voltage \times Current}\right) \quad (12)$$

After 10 minutes measurement for each system condition except conditions 4, 7, 10, more than 8000 system parameter data can be generated to obtain the box-plots, as shown in Figs. 6-7 which demonstrates the fuzzy-logic clustering of the system parameters obtained by FCM (as Eq. (2)). By Eq. (1), the results of the correlation coefficients matrix of the pumping system parameters are obtained and shown in Table 2.

The significant level matrix of the system parameters can be obtained and shown in Table 3. From Table 3, by adopting 95% confidence interval for the normal distribution, all the values in the significant level matrix less than 0.05 will be selected as the effective system parameters. The effective input parameters, as stipulated by the significant level matrix as depicted in Table 3, are voltage, current and power, whereas the effective output parameters are degree of vacuum, pressure and flow rate. Since the input power is dependent on voltage and current, only voltage and current are necessarily selected as the significant system input parameters.

After the determination of significant system input and output parameters, the fuzzy-logic clustering of the input-to-output parameter pairs for all running conditions is shown in Figs. 7(a)-7(f). Combining this significant parameter's clustering diagrams and the variation range of the box-plots for the system running conditions vs. each system parameter, the relations between system input and output parameters for faulty conditions can be detected as:

1. Pumping system for air-in mechanical fault performance refers to Figs. 6(a)-6(b) and Figs. 7(a)-7(b).

- An increase of air leak resulted in a reduction of the load current and an increase in the degree of vacuum.
- An increase in suction line clogging led to reduction of the load current and a raise in the degree of vacuum.
- An increase in discharge line clogging led to a reduced load current with a decrease of the degree of vacuum.

2. Pumping system for inlet-stuck mechanical fault performance refers to Fig. 6(a), 6(c) and Figs. 7(c)-7(d) are summarized as follows:

- Increase of air leak led to a reduction of the load current with a slight increase of the pressure.
- An increase in suction line and discharge line clogging led to a reduction of the load current with a slight decrease of the pressure.

3. Similarly, the pumping system for outlet-stuck mechanical fault performance refers to Fig. 6(a), 6(d) and Figs. 7(e)-7(f) are summarized as follows:.

- Increase in the air leak led to a reduction of the load current with a slight slow down of flow rate.
- Increase of the suction line clogging led to a reduction of the load current with no discernible influence on the stable flow rate.
- Increase of the discharge line clogging resulted in a reduction of the load current with the flow rate stabilized at a slower rate.

4. Comparing the electrical malfunction conditions 4, 7 and 10 with normal condition 1, the system parameter of current as displayed in Fig. 6 (a) and Fig. 7 (b) descended rapidly and the electricity disconnected under protection. No matter what the electrical malfunction condition was, the degree of vacuum as depicted in Fig. 6 (b) and Fig. 7 (b) remained almost the same and the pressure at the outlet as shown in Fig. 6 (c) and Fig. 7 (d) rose, but the flow rate as shown in Fig. 6 (d) and Fig. 7 (f) descended slightly.

3.3 Network architecture and diagnostic

Through the correlation analyses of the input and output parameter measurements, the input and output neuron vectors for BPN and RBF are of dimensions 2×1 (voltage and current) and 3×1 (degree of vacuum, pressure and flow-rate), respectively. The number of neurons of the hidden layer for FBPN is set to be 120 and 100 for CFBPN. For the RBF, the number of neurons in the hidden layer is increasing gradually up to the number of input measurements for each prescribed running condition. As shown in Figs. 8-9, the resolution of the clustering image of the measured data pairs in the state space of the pumping system input to ADALINE neural network is 1000×1000. The dimension of the output neuron vector of ADALINE is also 3×1. Such clustering images encompass the pairs for the degree of vacuum vs.

Table 1. Description of experimental conditions and channel label.

Sampling interval : 0.1, 0.08 & 0.01 second	
Channel ID & label	
1: Power factor (PF)	2: Voltage (input)
3: Current (input)	4: Power
5: RPM	6: Vacuum (output)
7: Pressure (output)	8: Flow rate (output)
Sampling conditions	
1: Normal condition	6: Inlet-stuck 3/3
2: Air-in 1/2	7: Open-phase
3: Air-in 1/4	8: Outlet-stuck 1/2
4: Frequency decay	9: Outlet-stuck 3/4
5: Inlet-stuck 1/2	10: Reverse-phase

pressure, pressure vs. flow rate and degree of vacuum vs. flow rate etc.; each pair has 10 running conditions, resulting in a total of 30 diagrams. These constitute the diagnosis database of the system. Parts of the measured data pairs are shown in Figs. 8-9, in which only the normal condition and air-in 1/2 condition are exhibited.

Part of the post linear regression coefficients analysis results for FBPN, CFBPN and RBF are listed in Table 4-6. Table 7 is part of the least mean square error results of the ADALINE network error. In these tables, the maximum post regression coefficients by BPN and RBF and the least mean square errors by

Table 2. Correlation coefficients matrix of pumping system parameters.

Input / Output	PF	Voltage	Current	Power	RPM	Vacuum	Pressure	Flow rate
PF	1.0000							
Voltage	-0.0006	1.0000						
Current	-0.0312	0.1481	1.0000					
Power	-0.0323	0.1309	0.5767	1.0000				
RPM	0.0047	-0.0198	-0.0194	-0.0158	1.0000			
Vacuum	-0.0195	-0.0471	-0.1813	-0.1517	-0.0454	1.0000		
Pressure	-0.0026	-0.0211	-0.2183	-0.2058	0.0340	-0.1841	1.0000	
Flow rate	-0.0073	0.0337	0.1764	0.1605	-0.0292	0.0206	-0.0778	1.0000

Table 3. Significant level matrix of pumping system parameters.

Input / Output	PF	Voltage	Current	Power	RPM	Vacuum	Pressure	Flow rate
PF	1.0000							
Voltage	0.9591	1.0000						
Current	0.0080	0.0000	1.0000					
Power	0.0061	0.0000	0.0000	1.0000				
RPM	0.6873	0.0931	0.0993	0.1791	1.0000			
Vacuum	0.0978	0.0001	0.0000	0.0000	0.0001	1.0000		
Pressure	0.8247	0.0734	0.0000	0.0000	0.0039	0.0000	1.0000	
Flow rate	0.5339	0.0042	0.0000	0.0000	0.0130	0.0798	0.0000	1.0000

Table 4. Post regression coefficients of system output for various condition by FBPN.

Running condition	Normal FBPN			Air in 1/2 FBPN			Air in 1/4 FBPN		
	V.	P.	F/R.	V.	P.	F/R.	V.	P.	F/R.
1: Normal Condition	0.8852	0.9796	0.9412	0.5199	0.8917	0.0774	0.5441	0.8016	0.8221
2: Air-in 1/2	-0.3327	0.8322	-0.1762	0.9181	0.9592	0.8635	0.5121	0.3633	0.1856
3: Air-in 1/4	0.4575	0.7065	0.3411	0.5553	0.8894	0.0590	0.9291	0.9656	0.9585
4: Frequency decay	0.4156	0.7503	-0.1535	-0.8811	-0.2345	-0.8937	-0.5969	0.6969	-0.1538
5: Inlet-stuck 1/2	0.3912	0.5935	0.2664	0.4362	0.7138	0.0791	0.3108	0.6202	0.7478
6: Inlet-stuck 3/3	0.0284	0.5224	-0.4499	0.2145	0.4110	-0.0218	0.2407	-0.1494	0.0329
7: Open-phase	0.5072	0.2976	0.2334	-0.6638	-0.4327	-0.9268	0.1234	0.7392	0.0800
8: outlet-stuck 1/2	0.2476	0.8342	0.3584	0.6225	0.7857	0.4286	0.5862	0.5606	0.5652
9: outlet-stuck 3/4	0.4679	0.8539	0.5890	0.5944	0.8693	0.1878	0.7542	0.7487	0.7837
10: Reverse-phase	0.6983	0.7263	0.3368	-0.7009	-0.3593	-0.8119	-0.4492	0.4855	-0.1014

where V is degree of vacuum, P is pressure and F/R is flow rate

Table 5. Post regression coefficients of system output for various condition by CFBPN.

Running condition	Normal CFBPN			Air in 1/2 CFBPN			Air in 1/4 CFBPN		
	V.	P.	F/R.	V.	P.	F/R.	V.	P.	F/R.
1: Normal Condition	0.8951	0.9783	0.9349	0.5023	0.8343	0.5485	0.6208	0.8423	0.7410
2: Air-in 1/2	0.2970	0.6689	-0.2594	0.9151	0.9585	0.8662	0.3171	0.6797	0.5774
3: Air-in 1/4	0.4638	0.7259	-0.0236	0.6102	0.7838	0.6226	0.9163	0.9615	0.9655
4: Frequency decay	-0.1533	0.4288	0.4766	-0.5517	0.8650	-0.5728	-0.3652	0.5883	-0.6641
5: Inlet-stuck 1/2	0.2918	0.5604	-0.0983	0.5620	0.5444	0.5123	0.2375	0.6726	0.6053
6: Inlet-stuck 3/3	0.4557	0.3997	0.2476	0.3614	0.2773	0.1718	0.1941	0.5086	0.6110
7: Open-phase	0.2152	0.4484	0.0552	-0.0692	0.4857	-0.5309	-0.1257	0.6293	-0.4079
8: outlet-stuck 1/2	0.4794	0.6709	-0.4543	0.4485	0.7259	0.2906	-0.1469	0.4459	0.5495
9: outlet-stuck 3/4	0.7038	0.8669	0.7486	0.5574	0.7946	0.6275	0.7472	0.7881	0.7204
10: Reverse-phase	0.5673	0.8446	-0.4997	-0.2424	0.7478	-0.6113	-0.7087	0.6870	-0.5832

where V is degree of vacuum, P is pressure and F/R is flow rate

Table 6. Post regression coefficients of system output for various condition by RBF.

Running condition	Normal RBF NN			Air in 1/2 RBF NN			Air in 1/4 RBF NN		
	V.	P.	F/R.	V.	P.	F/R.	V.	P.	F/R.
1: Normal Condition	0.8168	0.9711	0.8966	0.6427	0.6191	0.6454	-0.3929	-0.4229	-0.4322
2: Air-in 1/2	0.3447	-0.0253	0.2392	0.8834	0.9483	0.8270	-0.5298	-0.4202	-0.3925
3: Air-in 1/4	-0.2877	-0.3528	-0.3187	0.5377	0.6399	0.5291	0.8838	0.9571	0.9410
4: Frequency decay	0.0125	-0.4281	-0.4329	0.7831	0.5305	0.5504	-0.0202	-0.3029	-0.2915
5: Inlet-stuck 1/2	-0.2501	-0.4187	-0.4622	0.4596	0.4485	0.4992	0.3054	0.3757	0.3662
6: Inlet-stuck 3/3	-0.0453	0.0714	-0.0869	0.1747	-0.4281	0.2064	-0.0299	-0.5190	-0.0787
7: Open-phase	-0.2010	0.0889	0.2692	0.4949	0.5369	0.5072	-0.4122	-0.4386	-0.4125
8: outlet-stuck 1/2	-0.3202	-0.3774	-0.3272	0.4040	0.4532	0.3692	0.2484	0.2973	0.2197
9: outlet-stuck 3/4	-0.4015	-0.6022	-0.5432	0.5756	0.3615	0.3617	0.2826	0.1836	0.2732
10: Reverse-phase	0.5026	-0.0022	0.2481	0.0586	0.3663	0.3700	-0.7802	-0.7707	-0.8113

where V is degree of vacuum, P is pressure and F/R is flow rate

Table 7: Least mean square error of ADALINE network error after100 training epochs

Running condition	Condition 1 (Normal neural network)			Condition 2 (Air in 1/2 neural network)		
	V. vs. P.	P. vs. F/R.	V. vs. F/R.	V. vs. P.	P. vs. F/R.	V. vs. F/R.
1: Normal Condition	5.50845E-05	4.61804E-05	4.47682E-05	3.17029E-04	2.30082E-04	2.39732E-04
2: Air-in 1/2	3.49244E-04	1.82677E-04	2.40101E-04	5.46580E-05	4.96625E-05	4.52595E-05
3: Air-in 1/4	2.74660E-04	1.46006E-04	2.10551E-04	3.16370E-04	2.36347E-04	2.39076E-04
4: Frequency decay	3.30136E-04	1.57081E-04	2.23959E-04	3.13894E-04	2.36534E-04	2.38730E-04
5: Inlet-stuck 1/2	3.11592E-04	1.98533E-04	2.17306E-04	2.95390E-04	2.37463E-04	2.24792E-04
6: Inlet-stuck 3/3	3.50933E-04	1.99356E-04	2.42755E-04	1.80729E-04	2.38344E-04	1.72446E-04
7: Open-phase	3.52434E-04	1.96176E-04	2.42730E-04	3.13963E-04	2.36551E-04	2.39157E-04
8: outlet-stuck 1/2	3.44338E-04	1.71948E-04	2.37672E-04	3.21007E-04	2.19886E-04	2.43756E-04
9: outlet-stuck 3/4	3.48293E-04	1.95995E-04	2.39632E-04	3.19909E-04	2.36701E-04	2.41775E-04
10: Reverse-phase	3.52622E-04	2.00236E-04	2.42909E-04	3.24479E-04	2.38655E-04	2.45285E-04

ADALINE printed in gray background coincide with the neural network model, and can be used to characterize the system behavior and performance. So far, we have established 40 neural networks for the obvious diagnosis algorithm of the 10 system conditions. Corresponding to Tables 4-7, the regression diagnostic results can also be demonstrated by bar-charts (not shown).

3.4 Sensitivity analysis of output parameters

From the results of the sensitivity analysis of the output parameters, as listed in Table 8, it can be seen that for all ten system running conditions “pressure” is revealed to be the most significant parameter. Thus, it is most sensitive to observe the variation of pressure in the diagnosis process for the pumping system.

4. Conclusion

From the work and the results of the study, we can conclude that the analytical techniques of BPN, RBF, and ADALINE can be used to diagnose the mechanical pumping system successfully. From the analysis, we may conclude that:

The significant input/output neurons are determined to be (voltage, current)/ (degree of vacuum, pressure and flow-rate) by the methods of box-plot, fuzzy-logic clustering and correlation analysis for BPN and RBF. The significant data pairs are determined to be degree of vacuum vs. pressure, pressure vs. flow-rate and degree of vacuum vs. flow-rate used as input/output image neurons for ADALINE.

The judgment indices used for the purpose of diagnosis are determined by the maximum post regression value of parameters by correlation coefficient analysis between the neural network simulation and measurement results for both BPN and RBF. The diagnosis indices used by ADALINE are determined by the minimum values of the least mean square errors between the simulation and measurements vs. the prescribed normal and abnormal running conditions results.

Comparison of the three neural networks used in the mechanical pumping system, the BPN method has been determined to be the best in time-saving for learning followed by the ADALINE method and the RBF method by using the proposed neural network architectures. However, if the mechanical system diagnosis system is tackled off-line, the RBF method is suggested. Otherwise, for on-line diagnosis, the BPN method is recommended.

By the results of sensitivity analysis of the significant output parameters, the pressure variation should be surveyed first for the purpose of diagnosing the performance of the mechanical pumping system. It is obvious that if the pump system is situated in electrical fault conditions, the SNR of the pressure signal can be higher than 100 dB.

Table 8. Sensitivity analysis results for mechanical output parameters in dB.

Parameter / Condition	degree of Vacuum	Pressure	Flow rate
1: Normal Condition	6.0425	24.3763	12.2535
2: Air-in 1/2	11.0136	19.0192	6.7047
3: Air-in 1/4	11.0574	20.7493	17.7716
4: Frequency decay	71.0977	112.4026	91.5720
5: Inlet-stuck 1/2	4.9193	9.4882	11.3060
6: Inlet-stuck 3/3	5.8676	15.9225	9.7724
7: Open-phase	111.0220	121.5857	79.8474
8: outlet-stuck 1/2	14.1708	15.0860	13.8936
9: outlet-stuck 3/4	13.8649	20.3165	10.8974
10: Reverse-phase	201.8467	229.5293	123.9181

References

[1] C. R. Parten, R. Saeks and R. Pap, Fault Diagnosis and Neural Networks, Systems, Proceedings of IEEE Conference on Man and Cybernetics, Decision Aiding for Complex Systems, 3 (1991). 1517-1522.

[2] Chen, Wen-Chin and Chen, Chen-Tai, The Neural Network Implementation In Pattern Recognition Of Semiconductor Etching Process, *Journal of the Chinese Institute of Industrial Engineers*, 23 (4) (2006) 269-279.

[3] Chang, Chia-Tsang, Application of Neural Network and Genetic Algorithm to System Identification, *Thesis for the Master Degree*, (2003).

[4] K. Nam and S. Lee, Diagnosis of Rotating Machines by Utilizing a Back-Propagation Neural Net, Proceedings of the IEEE Conference on Industrial Electronics, Control, Instrumentation, and Automation, 1 (2) (1992)1064-1067.

[5] T. S. W. Chow and L. T. Law, Rotating Machines Fault Identification Using Back-Propagation Artificial Neural Network, Sixth International Conference on Electrical Machines and Drives, 412 - 415 (1993).

[6] K. L. Priddy, M. D. Lothers and R. E. Saeks, 1993, Neural networks and fault diagnosis in rotating machinery, IEEE Conference Proceedings on Systems, Man and Cybernetics, Systems Engineering in the Service of Humans, 2 (1993) 640-644.

[7] C. S. Pattichis and M. S. Pattichis, Adaptive Neural Network Imaging in Medical System, Thirty-Fifth Asilomar Conference on Signals, Systems and Computers, 1 (2001) 313-317.

[8] Z. H. Tzeng and J. G. Juang, Analysis and comparison of numeric identification using neural network, Proceedings of the Seventh Conference on Artificial Intelligence and Applications, (200) 396-401 (in Chinese).

[9] D. Zhang, A. Ghobakhlou and N. Kasabov, An Adaptive Model of Person Identification Combining Speech and Image Information, IEEE Conference on Control, Automation, Robotics and Vision, 1 (2004) 413-418.

[10] S. S. Young, H. Kwon, S. Z. Der and N. M. Nasrabadi, Adaptive Target Detection in Forward-Looking Infrared Imagery Using the Eigenspace Separation Transform and Principal Component Analysis, Society of Photo-Optical Instrumentation Engineers, 43 (8) (2004) 1767-1776.

[11] Cheng Wang, Yongle Xie and Guangju Chen, Fault diagnosis based on radial basis function neural network in analog circuits, *Communications, Circuits and Systems, IEEE Conference Proceedings*, 2 (2004) 1183-1185.

[12]Liang, H. and Lin, Z., Detection of Delayed Gastric Emptying from Electrogastrograms with Support Vector Machine, *IEEE Transactions on Biomedical Engineering* 48 (5) (2001) 601 – 604

[13] P. Singla, K. Subbarao and J. L. Junkins, Direction-Dependent Learning Approach for Radial Basis Function Networks, *IEEE Transactions on Neural Networks*, 18 (1) (2007) 203-222.

[14] Hsu, Zh-Chuan, Analyze and Forecast Mini Taiwan Stock Index Using Neural Network and Time Series, *Master degree thesis*, I-Shou University, (2005).

[15] D. R. Hush and B. G. Horne, Progress in supervised neural networks, *IEEE Signal Processing Magazine*, 10 (1) (1993) 8-39.

S. W. Piche, The selection of weight accuracies for Madalines, *IEEE Transactions on Neural Networks*, 6 (2) (1995) 432-445.

Tai-Ming Tsai, Lecture, Department of Marine Engineering, National Taiwan Ocean University PhD Candidate, Department of Systems Engineering and Naval Architecture, National Taiwan Ocean Uni-versity

Wei-Hui Wang Professor of emeritus and Director, Sound and Vibration Research Center Department of Systems Engineering and Naval Architecture, National Taiwan Ocean University PhD, Department of Mechanical and Marine Engineering, University of Plymouth, UK